

Article

Evaluation of Surface Mechanical Properties and Grindability of Binary Ti Alloys Containing 5 wt % Al, Cr, Sn, and V

Hae-Soon Lim ^{1,2}, Moon-Jin Hwang ³, Ha-Na Jeong ², Woon-Young Lee ³, Ho-Jun Song ³ and Yeong-Joon Park ^{3,*}

¹ Department of Dental Education, School of Dentistry, Chonnam National University, Gwangju 61186, Korea; hs1964@jnu.ac.kr

² Department of Dentistry, Chonnam National University Hwasun Hospital, Hwasun-gun, Jeonnam 58128, Korea; drhana28@hanmail.net

³ Department of Dental Materials and Medical Research Center for Biomineralization Disorders, School of Dentistry, Chonnam National University, Gwangju 61186, Korea; mjhwang@jnu.ac.kr (M.-J.H.); lwy11@jnu.ac.kr (W.-Y.L.); songhj@jnu.ac.kr (H.-J.S.)

* Correspondence: yjpark@jnu.ac.kr; Tel.: +82-62-530-4871

Received: 26 September 2017; Accepted: 6 November 2017; Published: 9 November 2017

Abstract: This study aimed to investigate the relationship between the surface mechanical properties and the grindability of Ti alloys. Binary Ti alloys containing 5 wt % concentrations of Al, Cr, Sn, or V were prepared using a vacuum arc melting furnace, and their surface properties and grindability were compared to those of commercially pure Ti (cp-Ti). Ti alloys containing Al and Sn had microstructures that consisted of only α phase, while Ti alloys containing Cr and V had lamellar microstructures that consisted of $\alpha + \beta$ phases. The Vickers microhardness of Ti alloys was increased compared to those of cp-Ti by the solid solution strengthening effect. Among Ti alloys, Ti alloy containing Al had the highest Vickers microhardness. At a low SiC wheel speed of 5000 rpm, the grinding rates of Ti alloys showed an increasing tendency as the hardness values of Ti alloys decreased. At a high SiC wheel speed of 10,000 rpm, the grinding rates of Ti alloys showed an increasing tendency as the tensile strength values increased. The Ti alloy containing Al, which showed the lowest tensile strength, had the lowest grinding rate. The grinding ratios of the Ti alloys were higher than those of cp-Ti at both wheel revolution speeds of 5000 and 10,000 rpm. The grinding ratio of the Ti alloy containing Al was significantly increased at 10,000 rpm ($p < 0.05$).

Keywords: Ti alloys; hardness; tensile strength; grinding rate; grinding ratio

1. Introduction

Titanium (Ti) has been used in dental prostheses, such as dental crowns, bridges, denture frameworks, and implant materials, due to its high specific strength, low elastic modulus, and good biocompatibility. Generally, Ti is cast into a specially formulated investment mold using a pressure-vacuum or high vacuum centrifugal casting machine to fabricate a prosthesis in the desired form. However, its high melting temperature (1668 °C) and chemical reactions with investment mold during the casting process result in brittle and hard α case formation on the surface, which make the finishing and polishing procedures difficult. To avoid problems during the casting process of Ti-based prostheses, the CAD/CAM technique was introduced in dentistry in the 1970s and developed rapidly for the convenient manufacture of dental prostheses. The clinical limitation of the CAD/CAM technique is that it is difficult to obtain precise restoration due to clinical parameters such as saliva, blood, or movements of the patient during oral structure scanning [1]. The other limitation is that the flaws on

the metal surface may be formed by the CAM milling process, and this negatively affects the strength and corrosion resistance. Additionally, a rough implant surface prepared by the CAD/CAM milling process is an important cause of ionic leakage and peri-implantitis [2]. Therefore, the ease of milling is an important requirement for dental CAD/CAM restorative materials. However, Ti is a fastidious metal for cutting during CAM manufacturing. Its intrinsic low thermal conductivity, high ductility, and chemical reactivity at high temperature [3,4] cause the Ti metal to have low grindability. A metal having low grindability is uneconomical because it takes more time to grind, and additional costs are needed to replace the grinding tools.

Because pure Ti has poor grindability, there have been many efforts to improve the grindability of Ti by alloying with various elements. Examples of these alloys include Ti-6Al-4V [5], Ti-Au, Ti-Ag [6], Ti-Cr [7,8], Ti-Cr-Cu [9], Ti-Zr [10–13], Ti-Cu [14], and Ti-Hf [15]. Grindability is defined as the relative ease of grinding a material. Grindability is affected by the material properties such as the microstructure, hardness, fracture toughness, elastic modulus, and ductility of Ti-based alloys, and by grinding conditions such as force, grinding tool materials and shape, workpiece feed speed, and tool revolution speed [16]. High speed grinding is recommended for increasing grinding efficiency and for reducing the formation of environmentally hazardous micro- and nanoparticles on the workpiece from chemical reactions at the cutting tool and the workpiece interface within a special temperature range [17]. Among the material properties of Ti alloys, it has been reported that reducing the ductility of Ti alloys is an effective way to improve grindability [6,18]. It has been reported that the formation of an intermetallic phase or a ω phase in the microstructure of Ti alloys resulted in reduced ductility and contributed to the improvement of grindability [7,14]. It is also reported that low fracture toughness and high elastic modulus are required to enhance grindability [4,19]. Meanwhile, a controversy exists with respect to the interpretation of the relationship between hardness and grindability. Takeyama et al. reported that higher strength and hardness of materials make the machining process more difficult [20]. On the other hand, Ho et al. reported that a Ti-40Zr alloy with higher microhardness had a higher grindability than that of a Ti-10Zr alloy with lower microhardness at a low grinding wheel speed [12]. It has been suggested by other researchers that hardness and strength are not the principal reasons for improved grindability [12,13,15]. Therefore, we investigated the effects of hardness on the grindability of cp-Ti and Ti alloys to obtain comprehensible information on this issue. Unlike the other related papers on the grindability of Ti alloys with increasing amounts of the same alloying elements [7–15,18,19], we tested the grindability of binary Ti alloys with different alloying elements.

Binary Ti-5 wt % (Al, Cr, Sn, and V) alloys were selected for testing the grindability because these alloys had microstructure, hardness, and tensile strength properties that were worth comparing, depending on their different alloy types and crystal phases. Even though Al and V elements are considered as having cytotoxic activity, according to the previous reports [21,22], binary Ti alloys with 5, 10, 15, and 20 wt % concentrations of the alloying elements (Al, Cr, Sn, and V) had a favorable cytocompatibility (cell viabilities > 80%), except for the Ti alloy containing 10 wt % V (cell viability = 66.9%).

This work aimed to investigate the effects of hardness and tensile strength on the grindability of binary Ti-5 wt % (Al, Cr, Sn, and V) alloys. Relatively low grinding tool speeds of 5000 rpm and 10,000 rpm were selected for grinding the Ti alloy. The Ti alloys were prepared using the arc-melting method and subsequent heat treatment. The cp-Ti and Ti alloy surfaces were characterized by X-ray diffractometry, optical microscopy, and scanning electron microscopy equipped with energy dispersive X-ray spectroscopy. Their mechanical properties were determined using a Vickers microhardness tester and a universal testing machine. The grindability of cp-Ti and Ti alloys was evaluated in terms of the grinding rate and grinding ratio.

2. Materials and Methods

Commercially pure Ti (cp-Ti, ASTM grade 2, Daito Steel Co. Ltd., Yaizu, Japan) was used as a control. Binary Ti alloys containing 5 wt % Al, Cr, Sn, and V were prepared using a vacuum arc melting system (SVT, Seoul Vacuum Tech Co. Ltd., Paju, Korea). Titanium sponge (99.95%), Al foil

(99.99%), Cr pieces (99.995%), Sn granules (99.99%), and V pieces (99.7%) were used as raw materials for the preparation of Ti alloys. All of these materials were purchased from Alfa Aesar (Ward Hill, MA, USA). Appropriate amounts of metals were placed in a water-cooled copper hearth in a chamber of the arc melting system. The chamber was evacuated to 1.33 mPa, and high purity Ar gas (99.9999%) was introduced until the pressure reached 26.67 kPa. Prior to melting the metals, pure Ti button was melted using a tungsten electrode to getter residual oxygen. The alloy ingots (15 g) were melted five times to ensure compositional homogeneity. Ti alloy ingots were subsequently heat-treated in a vertical tubular furnace under high purity Ar gas. The ingots were heated at a rate of 5 °C/min to a temperature that was 150 °C lower than their respective solidus temperatures [23] and were kept for 1 h. The heat-treating temperatures were 1570 °C for Ti-5Al, 1450 °C for Ti-5Cr, 1515 °C for Ti-5Sn, and 1500 °C for Ti-5V. After heat treatment, the ingots were cooled to 600 °C in a furnace at a rate of 10 °C/min and then air cooled to room temperature. The Ti alloy ingots were embedded in epoxy resin and cut to a 2 mm thickness using a low speed diamond saw. Ti alloy disks were progressively abraded using 100–2000 SiC grit papers and washed with acetone, ethanol, and distilled water.

In order to observe the microstructure, the surfaces of Ti alloys were mirror-polished using 0.3 µm Al₂O₃ powder and etched with Keller's reagent (H₂O:65% HNO₃:32% HCl:40% HF = 95:2.5:1.5:1.0). Metallographic observation of Ti alloys was carried out using an optical microscope (Epiphot FX-35WA, Nikon, Tokyo, Japan). The chemical composition was determined by an energy dispersive X-ray spectroscope (EMAX 7021-H, Horiba, Japan) attached to a scanning electron microscope (S-3000N, Hitachi Ltd., Tokyo, Japan).

The crystalline structure of Ti alloys was determined using an X-ray diffractometer (X'Pert PRO MPD, PANalytical B.V., Almelo, The Netherlands) with Cu K α radiation ($\lambda = 1.54056 \text{ \AA}$) at 40 kV and 40 mA.

The microhardness value of samples was measured using a Vickers microhardness tester (Zwick, Postfach4350, Ulm, Germany) with a load of 500 g for 30 s.

Tensile tests of samples were carried out using a universal testing machine (Instron 4302, Instron Co., Ltd., Buckinghamshire, UK) at a cross-head speed of 1.5 mm/min. Samples were made in reduced scale of ASTM E8 [24] using a wire cut electrical discharge machining (EDM) process. Prior to the tensile test, the specimen surfaces were polished with SiC papers up to 2000 grit. The overall dimension of the dumbbell-shaped specimen was 15 mm (L) \times 3 mm (W) \times 1.8 mm (T), and the dimension of parallel portion of the reduced section of the specimen was 4.88 mm (L) \times 1.5 mm (W) \times 1.8 mm (T). A specially fabricated grip assembly made of high grade carbon tool steel was used to hold the tensile test specimen to avoid a torsional force to the sample [25].

Figure 1 shows the grinding apparatus used in this study. Ti alloy disc samples were ground using an SiC wheel (703-120, Brasseler GmbH & Co., Lemgo, Germany) with a dimension of 1.5 mm thickness and 13.1 mm diameter attached to an electric handpiece of the dental motor (Strong 204, Saeshin, Daegu, Korea). A constant force of 100 gf was applied to the SiC wheel as the samples were ground [4,7–14]. The SiC wheel revolution speed was set to 5000 rpm and 10,000 rpm using a stroboscope (DX-525A, Seorim Electronics Co., Seoul, Korea).

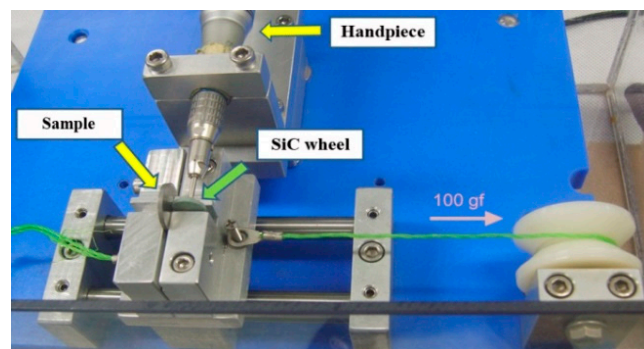


Figure 1. Grindability evaluation apparatus used in this study.

After the samples were ground for 1 min at two different speeds, their grinding rate and the grinding ratio were obtained by measuring the reduced volume of the samples and the SiC wheels. The reduced volume was calculated by multiplying the weight of the ground material by the density of the material obtained using Archimedes' principle. Before and after grinding, the weights of the samples and the SiC wheels were measured using an analytical balance with accuracy of 0.1 mg.

The ground surfaces and the ground metal chips were observed using a scanning electron microscope (S-3000N, Hitachi Ltd., Tokyo, Japan).

SPSS 21.0 version (SPSS, Inc., Chicago, IL, USA) was used to analyze the statistical significance. The statistical significance among samples was evaluated by one-way ANOVA with post hoc Duncan's multiple range tests with a significance defined at $p < 0.05$ level.

3. Results and Discussion

Figure 2 shows the X-ray diffraction patterns of samples. Compared to cp-Ti, reduced peak intensities of cast Ti alloys were attributed to slow furnace cooling during the heat treatment process. Reduced peak intensities of Ti alloys were adjusted by multiplying them by the appropriate number in order to compare phase composition with that of cp-Ti. Phase composition was affected by the alloying element type. Only an α Ti phase was observed in the Ti alloys containing an α -stabilizing element (Al) and a neutral element (Sn), while $\alpha + \beta$ Ti phases were observed in Ti alloys containing β -stabilizing elements (Cr and V) [26].

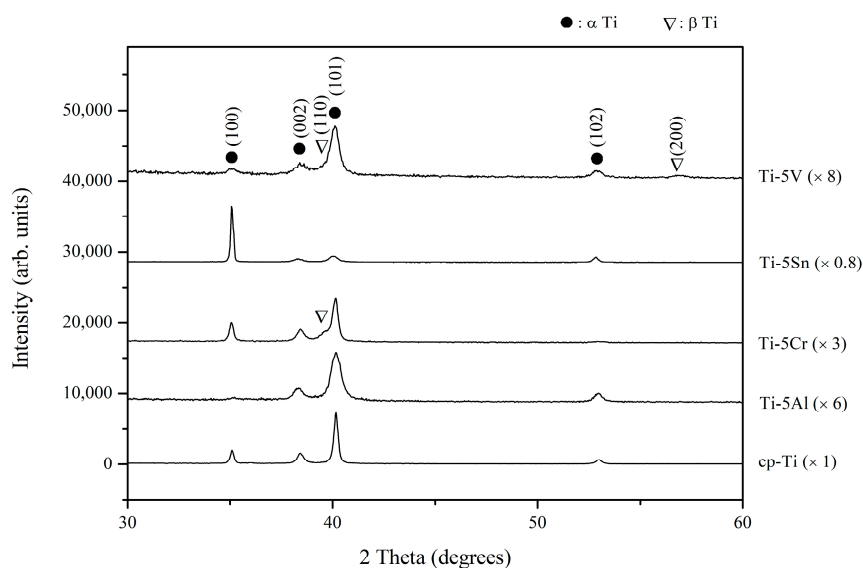


Figure 2. X-ray diffraction patterns of cp-Ti and Ti alloys (the peak intensities of Ti alloys were multiplied by the number in parentheses).

Figure 3 shows the optical microstructural images of samples at low magnification ($\times 100$). The microstructure of Ti alloys was changed by the alloying element type. The bright regions in the images shown in Figure 3 are etched areas on the sample surfaces. The cp-Ti had typical equiaxed grains ranging in sizes from 5 to 30 μm , while Ti-5Sn had irregular grain boundaries. Coarse columnar grain boundaries were observed in Ti-5Al. Ti-5Cr and Ti-5V displayed parallel lamellar microstructures, but their microstructural features were different. Ti-5Cr had a more acicular microstructure than Ti-5V. Table 1 lists the EDS elemental weight percentages of bulk, bright (marked as 'B'), and dark areas (marked as 'D') shown in Figure 3. Ti-5Al and Ti-5Sn did not show a significant difference in the alloying element content among bulk, bright, and dark areas. The 100 wt % Ti content was determined in the bright area of Ti-5Cr, while 97.8 wt % Ti content was determined in the bright area of Ti-5V. Dark areas of Ti-5Cr and Ti-5V were confirmed to be alloying element-rich areas.

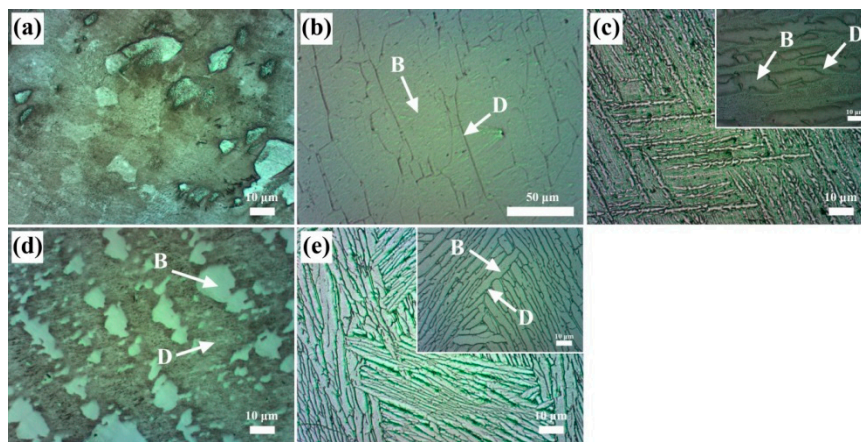


Figure 3. Optical microstructures of (a) cp-Ti; (b) Ti-5Al; (c) Ti-5Cr; (d) Ti-5Sn; (e) Ti-5V alloys. The micrographs of (a–e) are acquired with $\times 100$ and $\times 200$ objective, respectively. The insert images of (c,e) are the higher magnification ($\times 200$). The marked ‘B’ and ‘D’ mean the bright area and the dark area, respectively.

Table 1. The elemental weight percentages of Ti alloys shown in Figure 3.

Area	Elemental Weight %							
	Ti-5Al		Ti-5Cr		Ti-5Sn		Ti-5V	
	Ti	Al	Ti	Cr	Ti	Sn	Ti	V
Bulk	95.4	4.6	95.6	4.4	94.4	5.6	95.1	4.9
Bright	95.5	4.4	100	0	95.0	5.0	97.8	2.2
Dark	96.5	3.5	87.0	13.0	94.7	5.3	85.0	15.0

Table 2 lists the Vickers microhardness value of cp-Ti and Ti alloys. Vickers microhardness values of Ti alloys were increased compared to those of cp-Ti by the solid solution strengthening effect. Ti-5Al had higher Vickers microhardness (5.22 GPa) values because Ti-5Al has higher solid solution solubility than the other alloys according to the phase diagram of binary Ti alloys [23]. Ti-5Sn had a lower microhardness (3.36 GPa) value than Ti-5Cr and Ti-5V.

Table 2. Vickers microhardness values of cp-Ti and Ti alloys ($n = 5$).

Samples	Vickers Microhardness (GPa)
cp-Ti	1.52 ± 0.06 ^{a,*}
Ti-5Al	5.22 ± 0.19 ^e
Ti-5Cr	4.72 ± 0.28 ^d
Ti-5Sn	3.36 ± 0.60 ^b
Ti-5V	4.21 ± 0.22 ^c

* The superscript alphabets of a–e indicate significant differences between groups at the $p = 0.05$ level according to Duncan’s multiple range tests. Within the same column, the mean values with the same superscript alphabet are not statistically different ($p > 0.05$).

Table 3 lists the ultimate tensile strength and elongation values of cp-Ti and Ti alloys. The determined ultimate tensile strength (478.34 MPa) and elongation (42.28%) values of cp-Ti (Grade 2) were higher than the required values specified for cp-Ti (grade 2); 345 MPa and above 20%, respectively. Except for Ti-5V, which exhibited the highest ultimate tensile strength value of 845.54 MPa and a relatively high elongation value of 10.31%, Ti alloys had lower ultimate tensile strength values (78.57–362.83 MPa) and much lower elongation values (1.02–2.46%) than cp-Ti. The ultimate tensile strength values of Ti-5Al and Ti-5Sn were 78.57 MPa and 151.93 MPa, respectively.

Table 3. Ultimate tensile strength and elongation values of cp-Ti and Ti alloys ($n = 3$).

Samples	Ultimate Tensile Strength (MPa)	Elongation (%)
cp-Ti	478.34 ± 21.97 ^{d,*}	42.28 ± 2.83 ^c
Ti-5Al	78.57 ± 14.68 ^a	2.46 ± 1.16 ^a
Ti-5Cr	362.83 ± 75.95 ^c	1.02 ± 0.20 ^a
Ti-5Sn	151.93 ± 6.32 ^b	1.91 ± 0.47 ^a
Ti-5V	845.54 ± 3.96 ^e	10.31 ± 5.09 ^b

* The superscript alphabets of a–e for the ultimate tensile strength values and a–c for the elongation values indicate significant differences between groups at the $p = 0.05$ level according to Duncan's multiple range tests. Within the same column, the mean values with the same superscript alphabet are not statistically different ($p > 0.05$).

Figure 4 shows the grinding rates of cp-Ti and Ti alloys at SiC wheel revolution speeds of 5000 rpm and 10,000 rpm, which correspond to 206 m/min and 413 m/min, respectively. These SiC wheel speeds were lower than those in other studies (500–1250 m/min) [4,7–15]. Ti alloys displayed a reduced grinding rate at both wheel revolution speeds due to increased Vickers hardness. The grinding rates of metals increased with the increase in SiC wheel revolution speed, but the degree of increased grinding rate was different depending on the metal type. At 5000 rpm, the grinding rates of the metals were dependent on their Vickers hardness. Among the metals, higher Vickers hardness values of Ti-5Al and Ti-5Cr, as shown in Table 2, resulted in lower grinding rates (Figure 4a), while lower Vickers hardness values of Ti-5Sn and Ti-5V resulted in higher grinding rates (Figure 4a). The cp-Ti, which had the lowest Vickers hardness value, showed the highest grinding rate. At 10,000 rpm, the grinding rates of the metals were mainly affected by their ultimate tensile strength. Ti-5Al and Ti-5Sn, which had lower ultimate tensile strength values, showed lower grinding rates than cp-Ti, Ti-5Cr, and Ti-5V. It is noteworthy that Ti-5Al, which had the lowest ultimate tensile strength value, showed the lowest grinding rate. This result is different from the prediction that low ultimate tensile strength improves grindability [27].

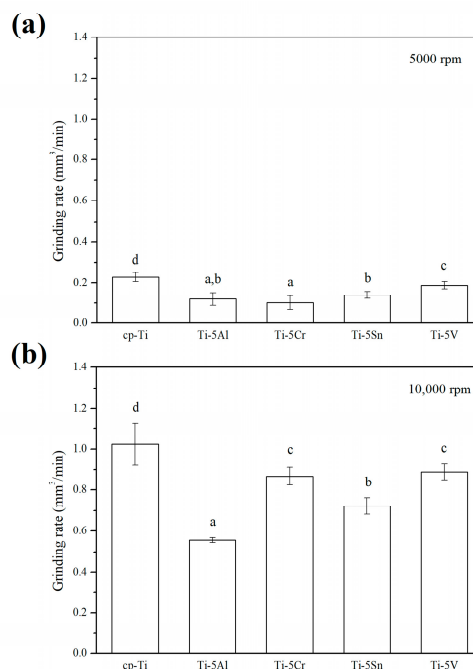


Figure 4. The grinding rates of cp-Ti and Ti alloys ground using an SiC wheel at revolution speeds of 5000 rpm and 10,000 rpm ($n = 7$). The superscript alphabets of (a) a–c and (b) a–d indicate significant differences at the $p = 0.05$ level according to Duncan's multiple range tests. The mean values with the same superscript alphabet are not statistically different ($p > 0.05$).

Figure 5 shows the grinding ratios of cp-Ti and Ti alloys at SiC wheel revolution speeds of 5000 rpm and 10,000 rpm. Compared to cp-Ti, Ti alloys showed higher grinding ratios, suggesting an increased tool life. At 5000 rpm, there was no significant difference between the grinding ratios of Ti alloys, but Ti-5Al and Ti-5Sn, consisting of an α phase, showed slightly higher grinding ratios than Ti-5Cr and Ti-5V, consisting of $\alpha + \beta$ phases. At 10,000 rpm, the grinding ratio of Ti-5Al was considerably high ($p < 0.05$), while the grinding ratios of the other Ti alloys were not significantly different between alloy groups. It was suggested that high Vickers hardness value and low ultimate tensile strength value of Ti-5Al resulted in the highest grinding ratio that could be expected for prolonged tool life.

Figure 6 shows the representative surface images of cp-Ti and Ti alloys ground at 5000 rpm and 10,000 rpm. At 5000 rpm, all ground metals displayed grinding marks and delaminated layers, as shown in the ground cp-Ti (Figure 6a), but the ground surface morphologies varied depending on the type of metal. The delaminated layers were mainly observed on the ground surfaces of cp-Ti and Ti-5Sn, while the ground metal particles were observed along with the delaminated layers on the ground surfaces of Ti-5Al and Ti-5Cr. The Ti-5V displayed a relatively smooth surface (Figure 6e). As the SiC wheel revolution speed increased from 5000 rpm to 10,000 rpm, the grinding marks were more clearly observed in all metals. At 10,000 rpm grinding, increased metal particle remnants were observed on the surfaces of all Ti alloys except for Ti-5V. More metal particles were observed on the ground surfaces of Ti-5Al, Ti-5Cr, and Ti-5Sn due to their low elongation (Table 3). At both grinding speeds, Ti-5V showed a smooth surface with few metal particle remnants, ensuring better ground surface quality.

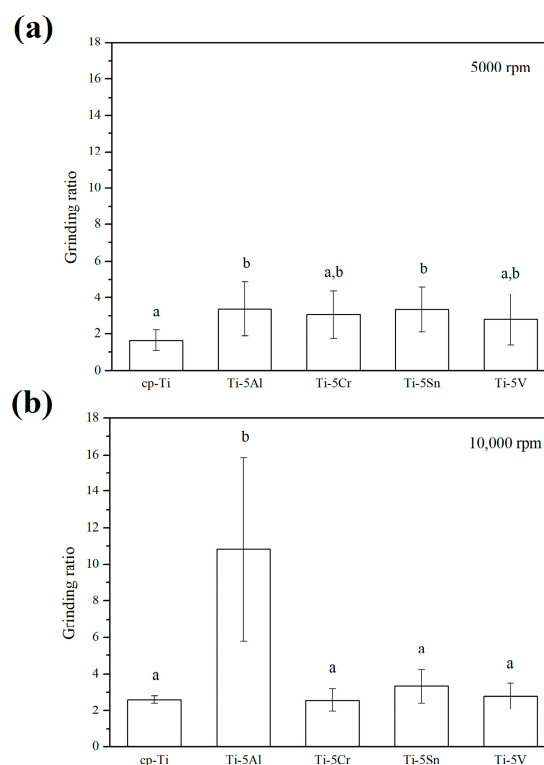


Figure 5. The grinding ratios of cp-Ti and Ti alloys ground using an SiC wheel at revolution speeds of 5000 rpm and 10,000 rpm ($n = 7$). The superscript alphabets (a,b) indicate significant differences at the $p = 0.05$ level according to Duncan's multiple range tests. The mean values with the same superscript alphabet are not statistically different ($p > 0.05$).

Figure 7 shows the metal chip images and SiC particles ground at 5000 rpm and 10,000 rpm. Even though a quantitative analysis was not performed for the sizes of metal chips and SiC particles,

their sizes were dependent on the type of metals. At 5000 rpm, the metal chip sizes of Ti alloys were smaller than those of cp-Ti, which had the lowest Vickers hardness value (1.52 GPa) (Table 2). Among the Ti alloys, Ti-5Al and Ti-5V showed relatively smaller metal chips, and Ti-5Sn showed larger metal chips, which can be ascribed to its low Vickers hardness value (3.36 GPa). As the SiC revolution speed was increased to 10,000 rpm, the shapes of the metal chips were dependent on the type of metals. The cp-Ti showed smaller metal chips at 10,000 rpm, while Ti-5Al, Ti-5Cr, and Ti-5V did not show distinct changes in the metal chip sizes obtained at 5000 rpm and 10,000 rpm. However, the Ti-5Sn had an increased metal chip size at 10,000 rpm, which might be attributed to the lower hardness and tensile strength values of Ti-5Sn compared to those of the other Ti alloys. Additionally, the small metal chips of Ti-5Al might be attributed to its lowest tensile strength and higher hardness values. In general, it is known that the smaller metal chips are more suitable for grinding Ti alloys [8]. However, Ti-5Al had lower grinding rates at 5000 rpm and 10,000 rpm. Despite the small metal chip formation, it was assumed that the decrease of grinding rates in Ti-5Al was due to the adhesion of metal particles on the grinding wheel surface, which worked to inhibit grinding [10].

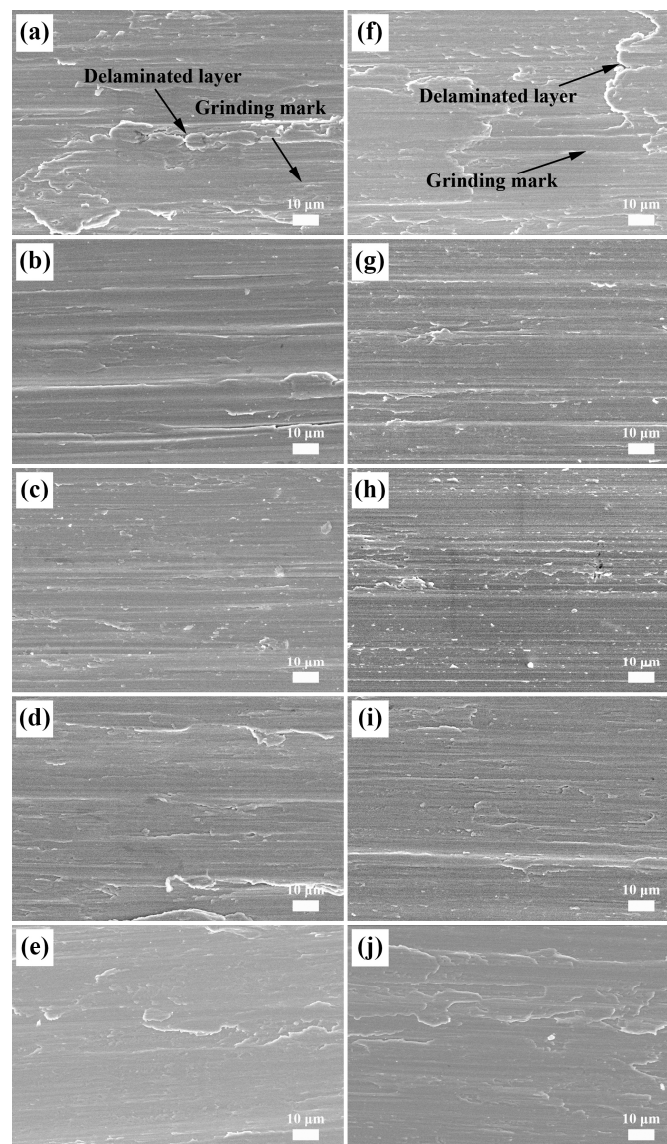


Figure 6. The surfaces of (a,f) cp-Ti; (b,g) Ti-5Al; (c,h) Ti-5Cr; (d,i) Ti-5Sn; (e,j) Ti-5V alloys ground using an SiC wheel at revolution speeds of 5000 rpm (left) and 10,000 rpm (right).

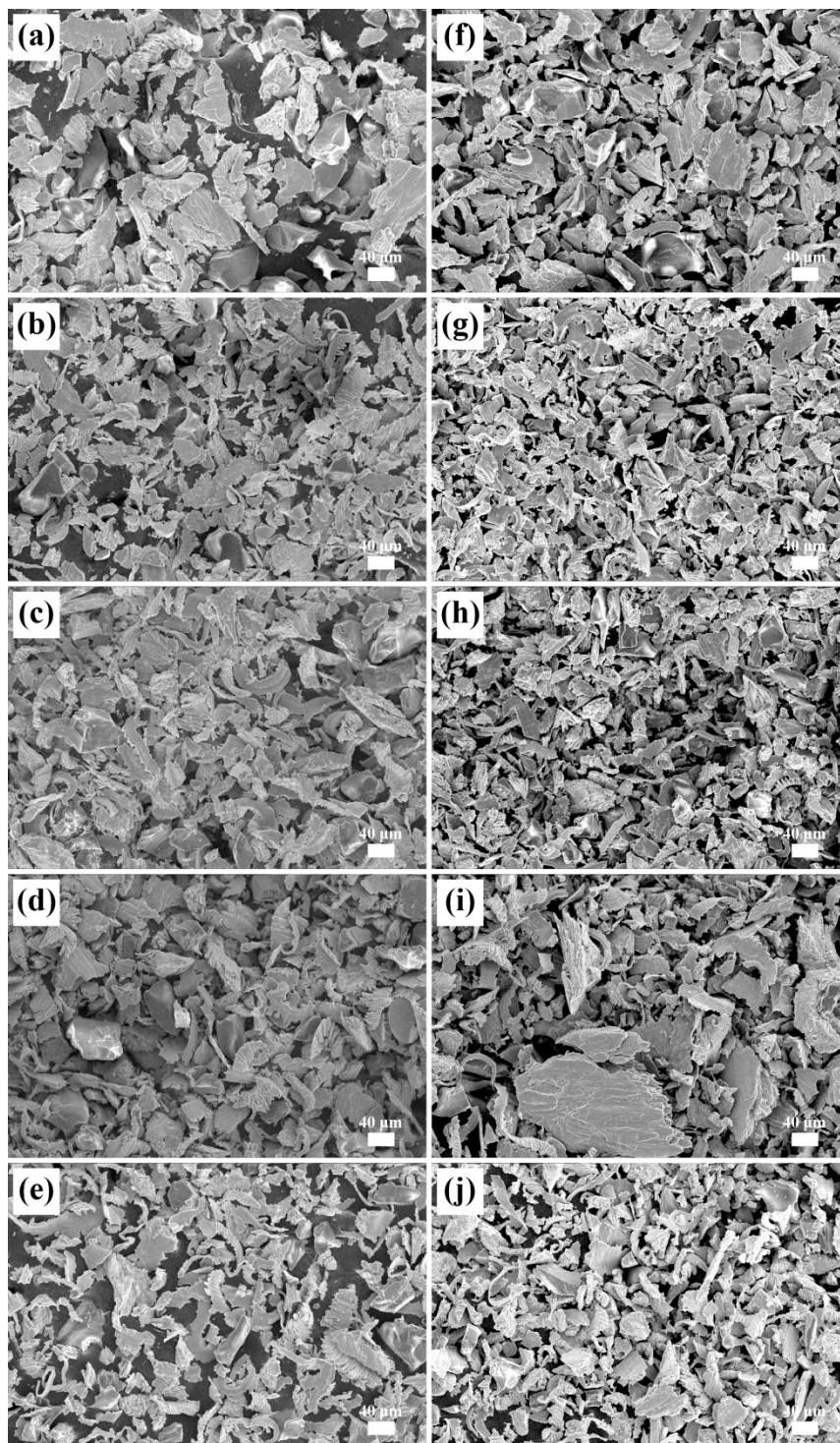


Figure 7. The ground particles of (a,f) cp-Ti; (b,g) Ti-5Al; (c,h) Ti-5Cr; (d,i) Ti-5Sn; (e,j) Ti-5V alloys ground using an SiC wheel at revolution speeds of 5000 rpm (left) and 10,000 rpm (right).

4. Conclusions

Binary Ti alloys containing 5 wt % Al, Cr, Sn, and V were prepared so that the relationship between mechanical properties and grindability could be investigated. At a low grinding speed of 5000 rpm, Ti-5Al and Ti-5Cr alloys, which had higher hardness values, showed lower grinding rates than Ti-5Sn and Ti-5V alloys, which had lower hardness values. The grinding ratios of Ti alloys showed

higher values compared to that of cp-Ti. At a high grinding speed of 10,000 rpm, the tensile strength became the contributing factor for the grinding rates of Ti alloys. Ti-5Cr and Ti-5V, which had higher tensile strength values, showed higher grinding rates than Ti-5Al and Ti-5Sn. Even though Ti-5Al and Ti-5Sn had substantially low ductility, the grinding rates were low due to their low ultimate tensile strength. Ti-5Al and Ti-5Sn, which had lower ultimate tensile strength, exhibited higher grinding ratios. Ti-5Al, which had the lowest ultimate tensile strength, exhibited the highest grinding ratio. There was a tendency for Ti alloys that had low ductility to leave more metal particles on the ground surfaces. The results obtained in this study are valuable for the development of Ti alloys that have good mechanical properties and grindability.

Acknowledgments: This work was supported by a National Research Foundation of Korea (NRF) grant funded by the Korea government (MSIP) (No. 2011-0030121), and by Chonnam National University (2015).

Author Contributions: Hae-Soon Lim and Moon-Jin Hwang designed and performed the experiments. Ha-Na Jeong and Woon-Young Lee analyzed the experimental data. The technical knowledge for binary Ti alloys was provided by Ho-Jun Song. The research work outlined in this paper was designed and supervised by Yeong-Joon Park.

Conflicts of Interest: The authors declare no conflict of interest.

References

1. Zarina, R.; Jaini, J.L.; Raj, R.S. Evolution of the software and hardware in CAD/CAM systems used in dentistry. *Int. J. Prev. Clin. Dent. Res.* **2017**, *4*, 1–8.
2. Palmquist, A.; Omar, O.M.; Esposito, M.; Lausmaa, J.; Thomsen, P. Titanium oral implants: Surface characteristics, interface biology and clinical outcome. *J. R. Soc. Interface* **2010**, *7*, S515–S527. [[CrossRef](#)] [[PubMed](#)]
3. Machado, A.R.; Wallbank, J. Machining of titanium and its alloys—A review. *Proc. Inst. Mech. Eng.* **1990**, *204*, 53–60. [[CrossRef](#)]
4. Kikuchi, M.; Takahashi, M.; Okabe, T.; Okuno, O. Grindability of dental cast Ti-Ag and Ti-Cu Alloys. *Dent. Mater. J.* **2003**, *22*, 191–205. [[CrossRef](#)] [[PubMed](#)]
5. Ohkubo, C.; Hosoi, T.; Ford, J.P.; Watanabe, I. Effect of surface reaction layer on grindability of cast titanium alloys. *Dent. Mater.* **2006**, *22*, 268–274. [[CrossRef](#)] [[PubMed](#)]
6. Chan, K.S.; Koike, M.; Okabe, T. Grindability of Ti alloys. *Metall. Mater. Trans. A* **2006**, *37*, 1323–1331. [[CrossRef](#)]
7. Hsu, H.C.; Wu, S.C.; Chinang, T.Y.; Ho, W.F. Structure and grindability of dental Ti-Cr alloys. *J. Alloys Compd.* **2009**, *476*, 817–825. [[CrossRef](#)]
8. Hsu, H.C.; Pan, C.H.; Wu, S.C.; Ho, W.F. Structure and grindability of cast Ti-5Cr-xFe alloys. *J. Alloys Compd.* **2009**, *474*, 578–583. [[CrossRef](#)]
9. Koike, M.; Itoh, M.; Okuno, O.; Kimura, K.; Takeda, O.; Okabe, T.H.; Okabe, T. Evaluation of Ti-Cr-Cu alloys for dental applications. *J. Mater. Eng. Perform.* **2005**, *14*, 778–783. [[CrossRef](#)]
10. Takahashi, M.; Kikuchi, M.; Okuno, O. Grindability of dental cast Ti-Zr alloys. *Mater. Trans.* **2009**, *50*, 859–863. [[CrossRef](#)]
11. Ho, W.F.; Wu, S.C.; Wang, H.W.; Hsu, H.C. Effects of Cr addition on grindability of cast Ti-10Zr based alloys. *Mater. Chem. Phys.* **2010**, *121*, 465–471. [[CrossRef](#)]
12. Ho, W.F.; Chen, W.K.; Wu, S.C.; Hsu, H.C. Structure, mechanical properties, and grindability of dental Ti-Zr alloys. *J. Mater. Sci. Mater. Med.* **2008**, *19*, 3179–3186. [[CrossRef](#)] [[PubMed](#)]
13. Ho, W.F.; Cheng, C.H.; Pan, C.H.; Wu, S.C.; Hsu, H.C. Structure, mechanical properties and grindability of dental Ti-10Zr-X alloys. *Mater. Sci. Eng. C* **2009**, *29*, 36–43. [[CrossRef](#)]
14. Kikuchi, M.; Takada, Y.; Kiyosue, S.; Yoda, M.; Woldu, M.; Cai, Z.; Okuno, O.; Okabe, T. Grindability of cast Ti-Cu alloys. *Dent. Mater.* **2003**, *19*, 375–381. [[CrossRef](#)]
15. Kikuchi, M.; Takahashi, M.; Sato, H.; Okuno, O.; Nunn, M.E.; Okabe, T. Grindability of cast Ti-Hf alloys. *J. Biomed. Mater. Res. Part B* **2006**, *77*, 34–38. [[CrossRef](#)] [[PubMed](#)]
16. Kalpakjian, S.; Schmid, S.R. *Manufacturing Engineering and Technology*, 7th ed.; Prentice Hall: Upper Saddle River, NJ, USA, 2013.

17. Khorasani, A.M.; Gibson, I.; Goldberg, M.; Nomani, J.; Littlefair, G. Machinability of metallic and ceramic biomaterials: A review. *Sci. Adv. Mater.* **2016**, *8*, 1491–1511. [[CrossRef](#)]
18. Okabe, T.; Kikuchi, M.; Ohkubo, C.; Koike, M.; Okuno, O.; Oda, Y. The grindability and wear of Ti-Cu alloys for dental applications. *J. Miner. Met. Mater. Soc.* **2004**, *56*, 46–48. [[CrossRef](#)]
19. Ho, W.F.; Wu, S.C.; Hong, Y.S.; Hsu, H.C. Evaluation of the machinability of Ti-Sn alloys. *J. Alloys Compd.* **2010**, *502*, 112–117. [[CrossRef](#)]
20. Takeyama, T.; Yoshikawa, T.; Takada, T. Study on machinability. *J. Jpn. Soc. Precis. Eng.* **1975**, *41*, 392–394.
21. Park, Y.J.; Song, Y.H.; An, J.H.; Song, H.J.; Anusavice, K.J. Cytocompatibility of pure metals and experimental binary titanium alloys for implant materials. *J. Dent.* **2013**, *41*, 1251–1258. [[CrossRef](#)] [[PubMed](#)]
22. Song, Y.H.; Kim, M.K.; Park, E.J.; Song, H.J.; Anusavice, K.J.; Park, Y.J. Cytotoxicity of alloying elements and experimental titanium alloys by WST-1 and agar overlay tests. *Dent. Mater.* **2014**, *30*, 977–983. [[CrossRef](#)] [[PubMed](#)]
23. Murray, J.L. *Phase Diagrams of Binary Titanium Alloys*; ASM International: Metals Park, OH, USA, 1987.
24. Holt, J.M. Uniaxial Tension Testing. In *Mechanical Testing and Evaluation, ASM Handbook*; ASM International: Materials Park, OH, USA, 2000; Volume 8.
25. Park, K.H.; Hwang, M.J.; Song, H.J.; Park, Y.J. Electrochemical and mechanical properties of cast Ti-V alloys for dental applications. *Int. J. Electrochem. Sci.* **2016**, *11*, 5552–5563. [[CrossRef](#)]
26. Peters, M.; Hemptenmacher, J.; Kumpfert, J.; Leyens, C. Structure and properties of titanium and titanium alloys. In *Titanium and Titanium Alloys. Fundamentals and Applications*; Leyens, C., Peters, M., Eds.; WILEY-VCH Verlag GmbH & Co. KGaA: Weinheim, Germany, 2003; pp. 1–36.
27. Chan, K.S.; Koike, M.; Okabe, T. Modeling wear of cast Ti alloys. *Acta Biomater.* **2007**, *3*, 383–389. [[CrossRef](#)] [[PubMed](#)]



© 2017 by the authors. Licensee MDPI, Basel, Switzerland. This article is an open access article distributed under the terms and conditions of the Creative Commons Attribution (CC BY) license (<http://creativecommons.org/licenses/by/4.0/>).